

Zinc oxide nanoparticle inhibits the biofilm formation of *Streptococcus pneumoniae*

Purnita Bhattacharyya · Bikash Agarwal · Madhurankhi Goswami · Debasish Maiti · Sunandan Baruah · Prosun Tribedi

Received: 5 April 2017 / Accepted: 17 August 2017 / Published online: 9 September 2017
© Springer International Publishing AG 2017

Abstract Biofilms are structured consortia of microbial cells that grow on living and non living surfaces and surround themselves with secreted polymers. Infections with bacterial biofilms have emerged as a foremost public health concern because biofilm growing cells can be highly resistant to both antibiotics and host immune defenses. Zinc oxide nanoparticles have been reported as a potential antimicrobial agent, thus, in the current study, we have evaluated the antimicrobial as well as antibiofilm activity of zinc oxide nanoparticles against the bacterium

Streptococcus pneumoniae which is a significant cause of disease. Zinc oxide nanoparticles showed strong antimicrobial activity against *S. pneumoniae*, with an MIC value of 40 µg/ml. Biofilm inhibition of *S. pneumoniae* was also evaluated by performing a series of experiments such as crystal violet assay, microscopic observation, protein count, EPS secretion etc. using sub-MIC concentrations (3, 6 and 12 µg/ml) of zinc oxide nanoparticles. The results showed that the sub-MIC doses of zinc oxide nanoparticles exhibited significant anti-biofilm activity against *S. pneumoniae*, with maximum biofilm attenuation found at 12 µg/ml. Taken together, the results indicate that zinc oxide nanoparticles can be considered as a potential agent for the inhibition of microbial biofilms.

Electronic supplementary material The online version of this article (doi:[10.1007/s10482-017-0930-7](https://doi.org/10.1007/s10482-017-0930-7)) contains supplementary material, which is available to authorized users.

Purnita Bhattacharyya and Bikash Agarwal contributed equally to this work.

P. Bhattacharyya · M. Goswami · P. Tribedi
Department of Microbiology, Assam Don Bosco University, Tapesia, Sonapur, Assam 782402, India
e-mail: purnitabhattacharyya@gmail.com

M. Goswami
e-mail: madhurankhigoswami@yahoo.com

B. Agarwal · S. Baruah (✉)
Department of Electronics & Communication Engineering, Assam Don Bosco University, Azara, Guwahati, Assam 781017, India
e-mail: sunandan.baruah@dbuniversity.ac.in

B. Agarwal
e-mail: bikash.agarwal@dbuniversity.ac.in

D. Maiti
Department of Human Physiology, Tripura University (A Central University), Suryamaninagar, Agartala, Tripura 799022, India
e-mail: debumaiti@gmail.com

P. Tribedi (✉)
Department of Biotechnology, The Neotia University, Sarisha, West Bengal 743363, India
e-mail: tribedi.prosun@gmail.com

Keywords *Streptococcus pneumoniae* · Zinc oxide nanoparticle · Antimicrobial · Anti-biofilm

Introduction

Traditional treatment processes against bacterial infections depend on the usage of different antimicrobial compounds or antibiotics that can either inhibit or kill growing microbial cells (Ojha et al. 2008). However pathogenic microorganisms are able to protect themselves against inhibitory compounds by the formation of biofilms (Johnson 2008). Biofilms are assemblages of microbial cells embedded in a matrix of self produced polymeric substances such as polysaccharides, protein and DNA. They are found adhering to both biological as well as non-biological surfaces (Oldak and Trafny 2005). Microbial biofilm formation involves four stages i.e. adhesion followed by microcolony formation, maturation and dispersion (Gupta et al. 2016). Among these, the process of dispersion in microbial biofilm formation is of high significance. This is because dispersion initiates a new infection cycle by colonising a new surface and thereby allowing the spread of infection (Kaplan et al. 2003). It has been reported that microbial biofilms are involved in chronic infectious diseases in humans, with estimates being around 65% of all infections according to the Centre for Disease Control (CDC) and 80% according to the National Institutes of Health (Joo and Otto 2012). Infectious diseases caused by biofilms include pneumonia, cystic fibrosis, periodontitis, endocarditis, osteomyelitis, rhinosinusitis and many more (Bjarnsholt 2013). Biofilms can also be seen in medical implants, urinary catheters and living tissues. Planktonic cells are free living cells that are typically susceptible to antimicrobials. When planktonic bacteria form biofilms, they can become resistant to antibiotics (Vasudevan 2014). Bacteria in biofilms are surrounded by an extracellular matrix that restricts the diffusion of antibiotics inside the biofilm and makes the microbial biofilm population resistant to antibiotics (Crossley et al. 2009; Thaya et al. 2016). Bacteria within biofilm shows reduced growth rates and secrete different surface molecules and virulence factors, which can enhance their pathogenicity by several hundred fold (Hall-Stoodley and Stoodley 2009).

Streptococcus pneumoniae, a biofilm forming Gram-positive bacterium is one of the most severe

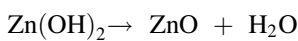
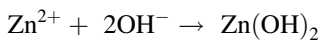
bacterial pathogens, causing a variety of serious diseases in humans such as community acquired pneumonia, bronchitis, meningitis and rhinosinusitis (Bogaert et al. 2004). *S. pneumoniae* is also responsible for chronic heart and lung disease in humans, mostly targeting infants below the age of 2 years and also adults above the age of 65 years (Ortvist et al. 2005; Chao et al. 2014). Thus, effective strategies must be adopted in order to combat the biofilm-linked diseases caused by *S. pneumoniae*. Nanotechnology has potential to complement conventional therapies against streptococcal infections due to their high efficacy and reliability (Markman et al. 2013). Currently, one of the most promising and novel therapeutic agents are nanoparticles because of their large surface area to volume ratio, charge density, low toxicity and higher specificity, resulting in a better degree of interaction with the bacterial cell (Vijayakumar et al. 2017). Zinc oxide (ZnO) nanoparticles have been widely used in healthcare commercial products due to their unique properties such as UV light absorption, being catalytic, semi-conducting, magnetic and antimicrobial nature (Vijayakumar et al. 2015). It has been reported that ZnO nanoparticles exhibit antimicrobial activity by rupturing the integrity of bacterial cell membrane, decreasing cell-surface hydrophobicity and down-regulating the transcription of oxidative stress resistance genes in bacteria (Pati et al. 2014). It has also been reported that ZnO nanoparticles possess strong anti-biofilm properties against *Pseudomonas aeruginosa* (Lee et al. 2014) but the biofilm attenuation activity by ZnO nanoparticles has not been investigated against *S. pneumoniae*. Therefore, in the current study, we have examined the effect of ZnO nanoparticles against the biofilm formation ability of *S. pneumoniae* and also explored the underlying mechanism behind the biofilm inhibition.

Materials and methods

Synthesis of ZnO nanoparticles

The nanoparticles were synthesised using the wet chemical method as described by Baruah et al. (2008). The synthesis of ZnO nanoparticles was done by first preparing solution A of 4 mM zinc acetate dihydrate $[\text{Zn}(\text{O}_2\text{CCH}_3)_2(\text{H}_2\text{O})_2]$ in 20 ml of 98% ethanol. Then solution A was rigorously stirred at 500 rpm at a

temperature of 50 °C for 45 min. Solution A was further diluted with 20 ml of 98% fresh ethanol under same stirring condition and temperature. Zinc acetate dihydrate dissociates to generate Zn^{2+} ions. Thereafter, solution B was prepared wherein 2 mM sodium hydroxide was prepared in 20 ml of 98% ethanol. Then solution B was added drop wise to cooled solution A at room temperature under mild stirring at 200 rpm for 5 min which makes the pH of the mixed solution 7.5. Upon addition of sodium hydroxide, OH^- ions are released. ZnO nanoparticles are formed through ionic reaction as given below:



The nanoparticle colloid was stabilised through an electrostatic stabilisation process of putting the solution in a hot water bath for 2 h at a temperature of 60 °C. Thereafter, the nanoparticle solution was dried to a powder form using a lyophilizer. The dried powder was then dissolved in sterile double distilled Milli Q water for experimental work.

Characterization of ZnO

The UV–visible absorption spectrum of the nanoparticle sample was measured in an ELICO-SL-159 spectrophotometer over the wavelength range of 200–800 nm. The synthesised ZnO nanoparticle samples were characterised for their crystal structure by X-ray diffraction (Rigaku D max-C) with $Cu\ K\alpha$ radiation to record the diffraction pattern. High resolution transmission electron microscopy (HRTEM) was performed with a JEOL JEM-3100F transmission electron microscope operated at 200 kV. The sample for TEM was prepared by placing a drop of the ZnO suspension in ethanol onto a standard carbon coated copper grid. The grids were dried before recording the micrographs. Energy dispersive spectroscopy (EDS) was used to confirm the elemental composition of the sample.

Microbial strain, growth media and culture conditions

S. pneumoniae MTCC 2672 used in this current study was provided by Dr. Debasish Maiti, Department of Human Physiology, Tripura University, India. In the

present study, *S. pneumoniae* was grown in Tryptic soy broth (TSB) medium at 37 °C for different lengths of time according to the experiment. For the preparation of TSB medium, pancreatic digest of casein (17 g), pancreatic digest of soya bean meal (3 g), sodium chloride (5 g), dibasic potassium phosphate (2.5 g), dextrose (2.5 g) were dissolved in sterilised 1 l Milli Q water and pH was then adjusted at 7.3 before sterilisation by autoclaving.

Determination of minimum inhibitory concentration by broth dilution assay

The minimum inhibitory concentration (MIC) of ZnO nanoparticles against *S. pneumoniae* was determined by using broth dilution method (Clinical and Laboratory Standards Institute 2005). An aliquot (10 μ l) of a culture of *S. pneumoniae* was added to sterile test tubes containing 5 ml of sterile TSB media. Thereafter, different concentrations of Zinc oxide nanoparticles (3, 6, 12 μ g/ml) were added to separate test tubes containing TSB media. In the control set, only the organism was grown in absence of ZnO nanoparticles. Subsequently, all the tubes including controls were incubated at 37 °C for 48 h. Thereafter, the MIC value was determined by observing growth.

Biofilm formation capability assessment by Crystal Violet method

Biofilm formation ability of *S. pneumoniae* was monitored by performing a crystal violet (CV) assay as described previously (Mukherjee et al. 2013; Tribedi and Sil 2014; Das et al. 2016). Briefly, 100 μ l of culture of *S. pneumoniae* was added into sterile test tubes containing 5 ml of sterile TSB. Subsequently, sub-MIC doses (3, 6, 12 μ g/ml) of ZnO nanoparticles were added to each test tube excluding the control set where only the organism was grown in absence of ZnO nanoparticles. All the test tubes were then incubated at 37 °C for 48 h. After the desired incubation time, the planktonic cells from each test tube were discarded and residual cells washed with sterile distilled water twice and dried adequately. Thereafter, in each tube, biofilms if any, were stained with 0.4% of CV solution for 15 min at room temperature. After that, the CV stain was poured off and tubes were washed with sterile distilled water once again. Then, 5 ml of 33% glacial acetic acid was added

in each tube in order to dissolve the adsorbed CV and the intensity of colour was quantified by measuring the absorbance at 420 nm.

Estimation of bacterial adhesion on Glass surfaces

The population density of *S. pneumoniae* on glass surfaces under different treatments was determined indirectly by measuring the concentration of extractable protein from the glass surface as the amount of extractable protein is directly proportional to the number of adherent microorganisms (Tribedi et al. 2015). To extract the protein from the adherent microorganisms on the glass surface, culture broths including the planktonic microorganisms were removed from both ZnO nanoparticle treated and untreated growth media after 2 days of incubation at 37 °C. All the test tubes were then washed with sterile Milli Q water, dried and then boiled for 30 min in 5 ml of 0.3 M NaOH. The suspension was then centrifuged at 8000 rpm for 10 min and the protein concentration of the supernatant was determined by the Lowry method (Lowry et al. 1951).

Visualization of biofilm morphology by microscopy

To confirm the results obtained from the CV assay, biofilm morphology was examined by microscopy. 100 µl of culture of *S. pneumoniae* was inoculated into sterile test tubes containing sterile TSB supplemented with different sub-MIC concentrations (3, 6, 12 µg/ml) of ZnO nanoparticles. In the control set, only the organism was allowed to grow without ZnO nanoparticles. Sterile cover slips were then added in each test tube and incubated at 37 °C for 48 h. After the desired incubation period, cover slips were aseptically taken out from each test tube and stained with CV and acridine orange (4 µg/ml) separately in order to examine the extent of biofilm association by light microscopy and fluorescence microscopy respectively.

Evaluation of growth curve

To evaluate the effect of ZnO nanoparticles on the growth of *S. pneumoniae*, a 100 µl of culture of *S. pneumoniae* was inoculated in conical flasks containing 100 ml of sterile TSB media. Following

inoculation, different sub-MIC concentrations (3, 6 and 12 µg/ml) of ZnO nanoparticles were added into each conical flask except the control set where only the organism was grown. All the conical flasks were then incubated at 37 °C for 48 h. At regular time intervals, the culture broth was separately taken from each growth media and absorbance was recorded at 600 nm in a colorimeter.

Cell viability measurement

To examine the viability of *S. pneumoniae*, we inoculated identical numbers of microorganisms ($\sim 1 \times 10^5$ CFU/ml) in sterile test tubes containing 5 ml of sterile TSB media and treated with different doses of ZnO nanoparticles at sub-MIC levels (3, 6 and 12 µg/ml). In the control set, ZnO nanoparticles were not added to the microorganisms. All the test tubes were then incubated at 37 °C for 48 h. For colony forming unit (CFU) calculation, 1 ml of culture media was separately collected from each conditioned media and diluted in 9 ml of sterile saline and thereafter serial dilutions were prepared. Thereafter, 100 µl of these diluted supernatants were plated onto solid TSB agar plates, incubated at 37 °C for 2 days and CFU were counted.

Extraction and measurement of Exopolysaccharides (EPS)

EPS secreted by the bacteria under nanoparticle treated and untreated condition was measured by following the protocol described by Tribedi and Sil (2013). In order to measure EPS under different conditions, 100 µl of culture of *S. pneumoniae* was inoculated in 30 mm polystyrene plates containing sterile TSB media supplemented with different doses of ZnO nanoparticles at sub-MIC levels (3, 6 and 12 µg/ml). In the control set, ZnO nanoparticles were added to the microorganisms. Sterile cover slips were added to the polystyrene plates. The plates were then incubated at 37 °C for 48 h. After incubation, the planktonic cells were discarded. The biofilm formed on the bottom of the polystyrene plates was recovered by scraping in sterile water. This biofilm suspension was then centrifuged at 6000 rpm for 20 min at 4 °C. After centrifugation, the supernatant was collected. The pellet was treated with 10 mM EDTA, vortexed for 15 min, and recentrifuged to extract cell-bound

exo-polysaccharides (EPS). The supernatant was collected and mixed with the previous supernatant. The pooled supernatants were then mixed with 2.2 volumes of chilled absolute ethanol and thereafter incubated at $-20\text{ }^{\circ}\text{C}$ for 1 h and centrifuged at 6000 rpm for 20 min at $4\text{ }^{\circ}\text{C}$. The pellet containing EPS was then collected and dissolved in sterile water. The amount of EPS formed was measured by the phenol–sulphuric acid method (Dubois et al. 1956).

Statistical analysis

Experimental results were subjected to statistical analysis of one-way analysis of variance (ANOVA). The relationship between ZnO nanoparticle sub-MIC doses, microbial attachment and extent of microbial biofilm formation was analysed by constructing contour plots using Minitab 16 software. The relationship between ZnO nanoparticle sub-MIC doses, EPS secretion and microbial biofilm formation was analysed by constructing contour plots using Minitab 16 software.

Results and discussion

Characterisation and identification of ZnO nanoparticles

Since nanoparticles have been considered as a potential agent for biofilm attenuation, in the current study, we synthesised ZnO nanoparticles in order to inhibit biofilm formation by *S. pneumoniae*. The nanoparticles were characterised through a series of experiments summarised in Fig. 1. Figure 1a shows the UV–Vis spectrum of ZnO nanoparticles in the wavelength range of 200–800 nm. Figure 1b shows the plot of $(\alpha h\nu)^2$ versus photon energy ($h\nu$) of ZnO nanoparticles using Tauc's relation. The band gap energy value for ZnO samples was calculated from this plot. The wavelength of 380 nm corresponds to a bulk band-edge of 3.37 eV for ZnO. The band gap as calculated from Fig. 1b is 5.54 eV, indicating the presence of nano-crystallites. The absorbance at wavelength of 280 nm indicates a blue shift, and an increment in the band gap energy, which should be due to the quantum confinement effect from the small particles of size 10 nm as found in XRD analyses. A TEM micrograph of the ZnO nanoparticles is shown in Fig. 1c. The

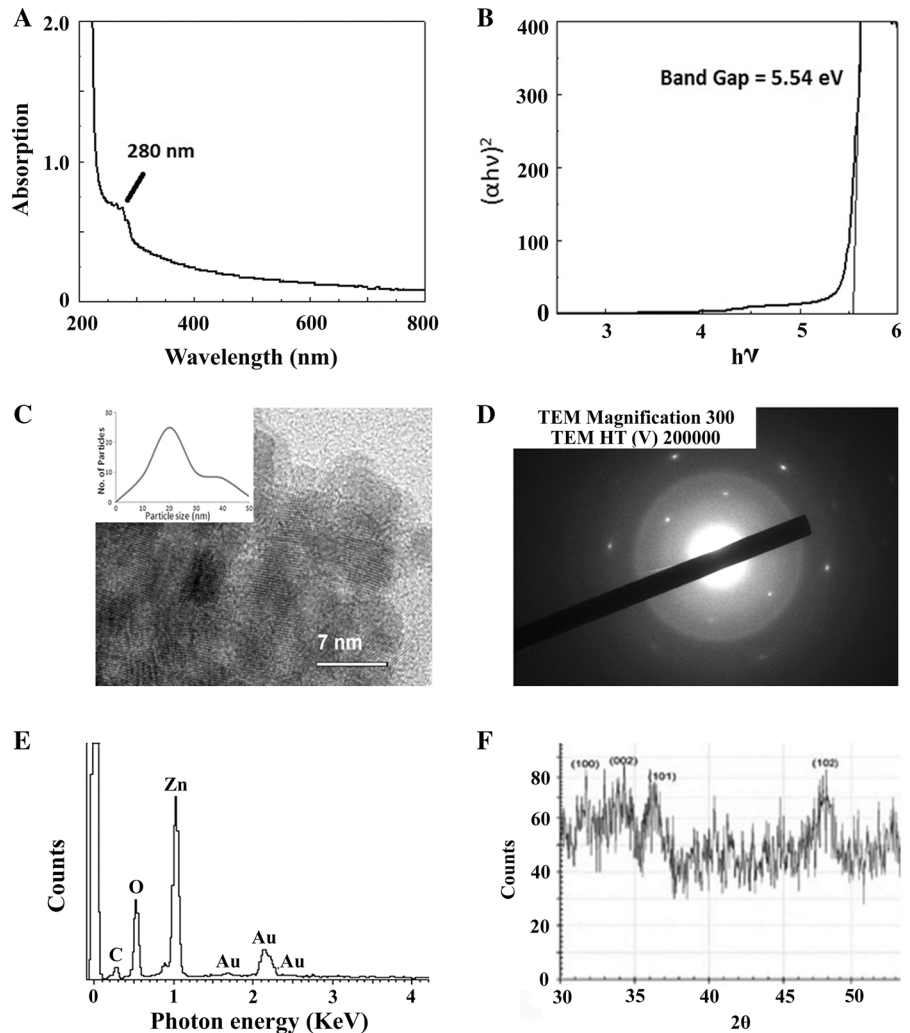
shape of ZnO nanoparticles as observed is nearly spherical agglomerated into polycrystalline structures of different sizes. The smallest size of the ZnO nanoparticles is about 8 nm whereas the average size of the nanoparticles is around 15 nm. The inset shows a particle size distribution from a sample of 50. Figure 1d shows the selected area electron diffraction in which distinct bright rings indicates single crystalline behaviour. The rings around the central beam are because of diffraction from different closely packed nanoparticles, giving an overall polycrystalline effect. The energy dispersive spectra as shown in Fig. 1e clearly shows that the sample prepared by the hydrothermal method has a pure ZnO phase. The XRD pattern of the ZnO nanoparticles is shown in Fig. 1f. All XRD diffraction peaks of ZnO powders are in good agreement with a hexagonal structure of zincite phase reported in JCPDS File Card No.05-0664. No peaks of impurity were observed, indicating the high purity of the synthesised ZnO. The particle size was calculated using Debye–Scherrer formula $D = K\lambda/(\beta\cos\theta)$, where K is Scherrer constant, λ is the X ray wavelength, β is the peak width of half maximum, and θ is the Bragg diffraction angle. The average crystallite size D is 15 nm, calculated using the Debye–Scherrer formula. The peaks at scattering angles (2θ) of 31.64° ,

34.85° , 36.65° and 47.53° which corresponds to (100), (002), (101) and (102) crystal planes respectively. It also shows that the particle has a hexagonal phase (wurtzite structure) with lattice constants $a = b = 3.2492\text{ \AA}$, $c = 5.20661\text{ \AA}$.

Antimicrobial activity of ZnO nanoparticles against *S. pneumoniae*

Since ZnO nanoparticles have been reported as a potential antimicrobial agent against different microorganisms (Salem et al. 2015), this study aimed to determine the antimicrobial activity of ZnO nanoparticles against *S. pneumoniae*. A broth dilution system test, wherein the ZnO nanoparticles were solubilised in sterile double distilled water, was used for the determination of the minimum inhibitory concentration (MIC). This test was selected to overcome the solubility and diffusion problems of ZnO nanoparticles in agar diffusion methods. The MIC is defined as the lowest concentration of an antimicrobial agent at which there is no visible growth of the

Fig. 1 Characterisation of ZnO nanoparticles. **a** UV–vis spectra of ZnO nanoparticles. **b** Plot of $(\alpha h\nu)^2$ versus Photon energy ($h\nu$) of ZnO nanoparticles using Tauc's relation. **c** TEM micrograph of the ZnO nanoparticles. **d** Selected area electron diffraction of ZnO nanoparticles. **e** Energy dispersive spectra of ZnO nanoparticles. **f** XRD pattern of ZnO nanoparticles



bacteria after the desired time of incubation. The result showed that ZnO nanoparticles exhibited strong antimicrobial activity against *S. pneumoniae*, with an MIC value of 40 $\mu\text{g/ml}$.

Anti-biofilm activity of ZnO nanoparticles against *S. pneumoniae*

The involvement of biofilms in microbial infections can increase the pathogenicity of the microorganism and protect the microorganism from being destroyed by external treatments (Gupta et al. 2016). Biofilm-associated bacteria often exhibit antibiotic resistance (Vasudevan 2014), reduced growth rate and secretion of virulence factors (Hall-Stoodley and Stoodley

2009). Thus, efficient strategies are urgently required for preventing the development of harmful biofilms. After determining the antimicrobial effectiveness of ZnO nanoparticles against *S. pneumoniae*, we examined their possible anti-biofilm activity. To determine the anti-biofilm activity of ZnO nanoparticles against *S. pneumoniae*, 100 μl of cultures of *S. pneumoniae* were inoculated into sterile test tubes containing TSB. Varying sub-MIC concentrations (3, 6, 12 $\mu\text{g/ml}$) of ZnO nanoparticles were added and incubated at 37 °C for 48 h. After incubation, planktonic cells were discarded from each growth, including the control where the microorganism was not treated with ZnO nanoparticles. The biofilm microbial population on the glass tube surface was then stained with CV solution.

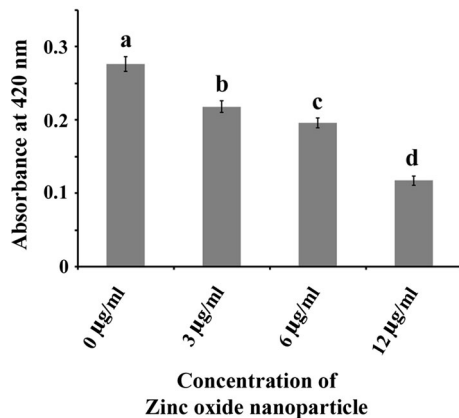


Fig. 2 Crystal violet staining of biofilm formation. Biofilms were formed in the presence and absence of ZnO nanoparticles and quantified by CV staining. Error bars indicate standard deviation (\pm SD) of replicates. Statistical significance between the groups was evaluated by ANOVA at 5% level

The results showed that ZnO nanoparticles exhibit moderate to significant anti-biofilm properties against *S. pneumoniae* compared to the control (Fig. 2). The extent of microbial biofilm formation in test tubes in the presence and absence of ZnO nanoparticles was also measured by determining the amount of total extractable protein (Balasubramanian et al. 2010; Tribedi and Sil 2013). Since it is very hard to estimate the total microbial populations on the test tube surfaces by conventional plate counting, total protein extraction can be another tool to count the extent of the microbial population on the glass surfaces. We observed less protein from those test tubes where microorganisms were treated with ZnO nanoparticles compared to control tubes where the microorganisms were grown in the absence of ZnO nanoparticle (Fig. 3). Thus, the results suggest that treatment with ZnO nanoparticles, reduced attachment to the glass surface preventing biofilm formation.

ZnO nanoparticles inhibit microbial attachment

Bacterial biofilm formation is accomplished in several stages including attachment, micro-colony formation, maturation and dispersion. One likely explanation for microbial biofilm attenuation by ZnO nanoparticles could be the prevention of bacterial attachment to the surfaces as this is the initial step of biofilm formation (Lau et al. 2009). To test this, 100 μ l culture of *S. pneumoniae* was inoculated in sterile TSB media containing sterile cover slips. Sub-MIC doses of ZnO

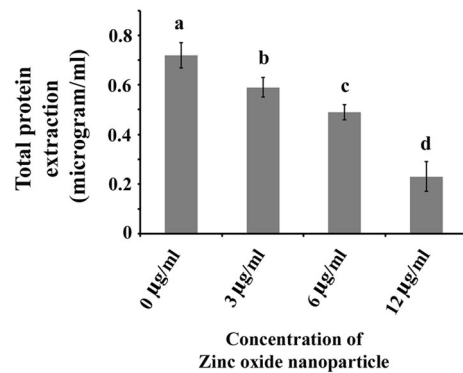


Fig. 3 Total protein extraction profile as a measure of biofilm formation. Biofilms were formed in the presence and absence of ZnO nanoparticles. Adherence of *S. pneumoniae* to the walls of the test tubes was estimated by measuring the total extractable protein. Error bars indicate standard deviation (\pm SD) of replicates. Statistical significance between the groups was evaluated by ANOVA at 5% level

nanoparticles (3, 6, 12 μ g/ml) were then added to the growth media and incubated at 37 °C for 48 h. After the incubation, cover slips were removed from the growth media, stained with CV and acridine orange to observe the biofilms under light and fluorescence microscope respectively. In the control set, microorganisms were grown in the absence of ZnO nanoparticles. We observed that, in the control set, *S. pneumoniae* showed a very dense microbial biofilm network on the glass surface (Fig. 4a, b). However, in case of the ZnO nanoparticles treated samples, the result showed that microorganisms reduced colonisation of the cover slip surfaces, with maximum and minimum reduction in the microbial attachment observed at 12 and 3 μ g/ml concentration of ZnO nanoparticles respectively (Fig. 4a, b). In order to validate this correlation between the sub-MIC doses of ZnO nanoparticles, microbial attachment and biofilm formation, we constructed a contour plot as a graphical representation of the relationships among three numeric variables in two dimensions (Fig. 5). Consistent with our expectation, the contour plot demonstrated that the sub-MIC doses of ZnO nanoparticles attenuate microbial attachment and formation of biofilm considerably (Fig. 5). Taken together, the results clearly demonstrate that the treatment of *S. pneumoniae* with ZnO nanoparticles reduces the microbial colonization of glass surfaces considerably, resulting in the inhibition of microbial biofilm formation.

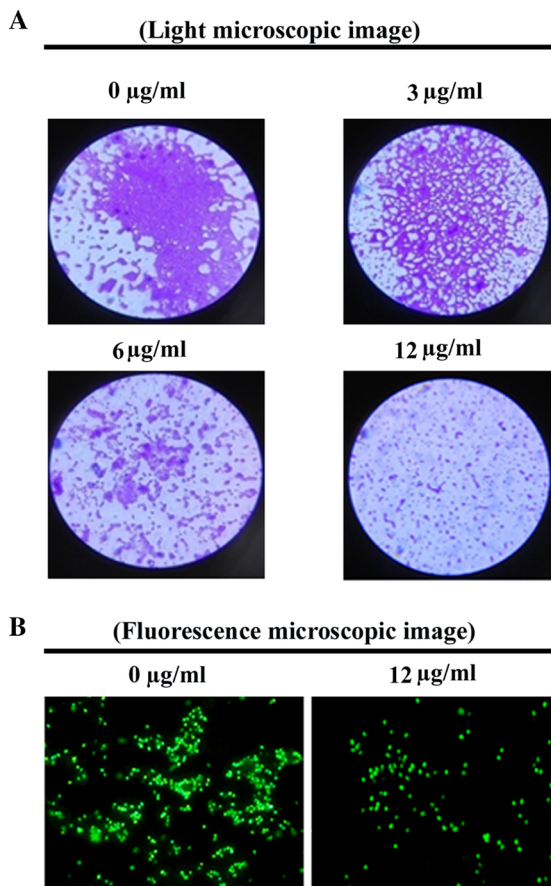


Fig. 4 Micrographs of *S. pneumoniae* biofilms. Adherence of *S. pneumoniae* to cover slips recovered from growth media supplemented with different doses of ZnO nanoparticles was examined by staining with CV and acridine orange. **a** CV stained cover slips were observed by light microscopy. **B**. Acridine orange stained cover slips were observed by fluorescence microscopy. Both figures are representative of images obtained from 20 different fields for each group and from three independent experiments

Sub-MIC doses of ZnO nanoparticles do not affect the microbial cell viability

To examine the effect of the sub-MIC doses of ZnO nanoparticles on the growth of *S. pneumoniae*, we incubated the bacteria with different sub-MIC doses (3, 6 12 µg/ml) of ZnO nanoparticles and compared the growth profile of the bacteria with the control where the organism was grown in absence of ZnO nanoparticles. During the course of incubation, we aseptically collected equal volumes of culture from both nanoparticle treated and untreated sets at regular time intervals and recorded the OD at 600 nm. The

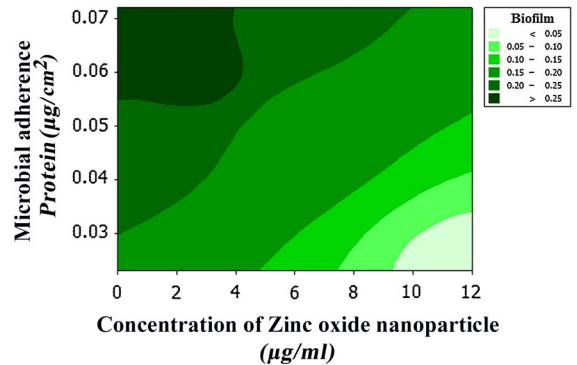


Fig. 5 Contour plot of biofilm versus cellular attachment and ZnO nanoparticles. The plot was constructed using Minitab 16 software. Different colours represent different degrees of biofilm formation

results showed that there was no major difference in the growth pattern of the bacteria between the treated and untreated conditions (Fig. 6a). We also compared the viable microbial cell count between ZnO nanoparticle treated and untreated growth media by plating 100 µl of the bacterial cultures. After incubation in identical condition, we observed no significant differences in CFU between ZnO treated and untreated culture media (Fig. 6b). Thus, the results showed that all the tested sub MIC doses (3, 6 and 12 µg/ml) of ZnO nanoparticles do not exhibit cell killing or growth arresting properties but they do interfere with biofilm formation.

ZnO nanoparticles inhibit bacterial EPS production

Secretion of EPS from microorganism can stabilise complex biofilm structures efficiently (Flemming and Wingender 2010). Besides, EPS is one of the major mechanisms of drug resistance for the microbial biofilm. Thus EPS attenuation is also considered as one of the major inhibitors of biofilm formation (Tribedi and Sil 2013). Therefore, we examined the effect of different doses (3, 6 and 12 µg/ml) of ZnO nanoparticles on the EPS secretion by *S. pneumoniae*. Consistent with other earlier results, we noticed that EPS secretion from the bacteria was significantly reduced when organisms were treated with the sub-MIC doses (3, 6 and 12 µg/ml) of ZnO nanoparticles compared to the untreated controls (Fig. 7). Moreover,

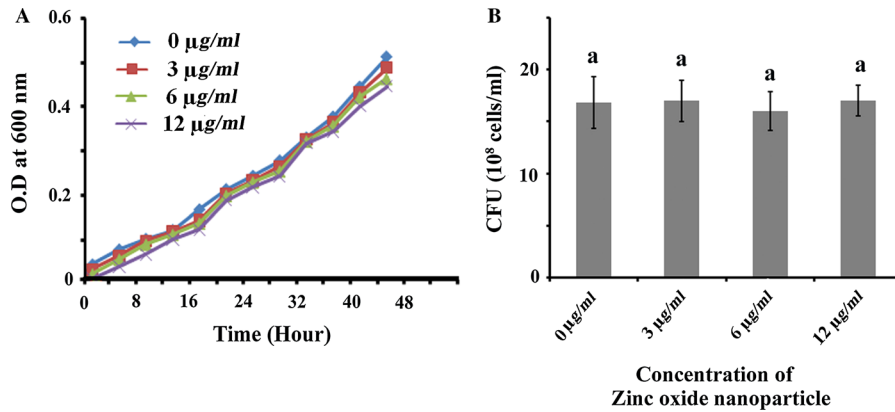


Fig. 6 Cell viability assays. **a** Growth curve analysis. Bacteria were grown in media supplemented with varying concentrations of ZnO nanoparticles and growth measured as absorbance at 600 nm. Three replicates were used for each experimental set. Error bars indicate standard deviation (\pm SD). **b** Colony forming unit (CFU) assay. CFU were counted from both ZnO

nanoparticle treated and untreated culture media after 48 h of incubation at 37 °C. Three replicates were performed for each experimental set. Error bars indicate standard deviation (\pm SD). Statistical significance between the groups was evaluated by ANOVA at 5% level. Mean values with the same letters are significantly similar among the treatments

we found that the maximum reduction in EPS count was observed at 12 µg/ml concentration of ZnO nanoparticles (Fig. 7). Taken together, these results indicate that the tested sub-MIC doses (3, 6 and 12 µg/ml) of ZnO nanoparticles exhibit moderate to significant biofilm attenuation activity against *S. pneumoniae*. In order to examine the correlation between EPS

secretion and biofilm formation, we constructed a contour plot comparing ZnO nanoparticle doses, EPS secretion and biofilm formation. The result showed that when EPS secretion is high, microbial biofilm formation was favoured and vice versa (Fig. 8). The result also showed that with the increase in sub-MIC doses (3, 6 and 12 µg/ml) of ZnO nanoparticles, EPS secretion considerably decreases, which may explain the reduction in microbial biofilm formation (Fig. 8). Taken together, these results clearly demonstrate that ZnO nanoparticles efficiently work as an anti-biofilm agent against *S. pneumoniae*.

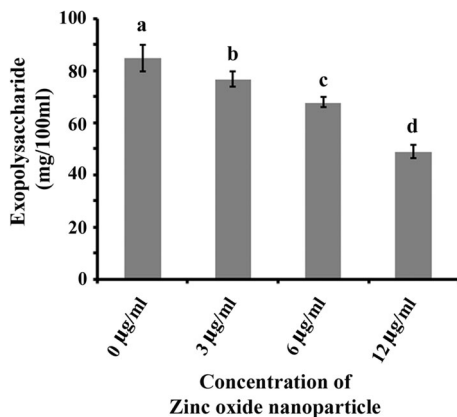


Fig. 7 Exo-polysaccharide (EPS) secretion profile. EPS was extracted from both ZnO nanoparticle treated and untreated growth media and measured by the phenol–sulphuric acid method. The result represents the average of three independent experiments. Error bars indicate standard deviation (\pm SD). Statistical significance between the groups was evaluated by ANOVA at 5% significance level. Mean values with different letters are significantly different between the treatments

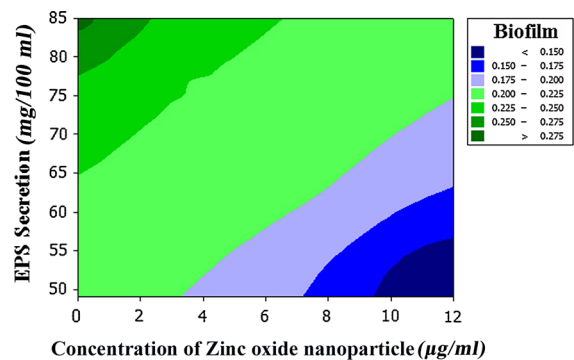


Fig. 8 Contour plot of biofilm versus EPS and ZnO nanoparticles. The plot was constructed using Minitab 16 software. Different colours represent different degrees of biofilm formation

Conclusion

Introduction of biofilm attenuating agents may allow therapeutic approaches against biofilm-associated human infections. Our current study demonstrates that sub-MIC doses (3, 6 and 12 µg/ml) of ZnO nanoparticles exhibit efficient anti-biofilm activity against *S. pneumoniae*. Thus, ZnO nanoparticles may work as part of a combination therapy against drug resistant *S. pneumoniae* infections, where biofilm formation plays a crucial role in disease progression.

Acknowledgements The authors would like to express sincere gratitude to the learned reviewers for their valuable comments raised during the course of review for the betterment of the quality of the current research work.

Conflict of interest Authors declare that they do not have any conflict of interest.

References

- Balasubramanian V, Natarajan K, Hemambika B, Ramesh N, Sumathi CS, Kottaimuthu R, Rajash KV (2010) High-density polyethylene (HDPE)-degrading potential bacteria from marine ecosystem of Gulf of Mannar, India. *Lett Appl Microbiol* 51(2):205–211
- Baruah S, Rafique RF, Dutta J (2008) Visible light photocatalysis by tailoring crystal defects in zinc oxide nanostructures. *NANO* 3(05):399–407
- Bjarnsholt T (2013) The role of bacterial biofilms in chronic infections. *Apmis* 121(s136):1–58
- Bogaert D, de Groot R, Hermans PWM (2004) *Streptococcus pneumoniae* colonization: the key to pneumococcal disease. *Lancet Infect Dis* 4(3):144–154
- Chao Y, Marks LR, Pettigrew MM, Hakansson AP (2014) *Streptococcus pneumoniae* biofilm formation and dispersion during colonization and disease. *Front Cell Infect Microbiol* 13:4
- Clinical and Laboratory Standards Institute (2005) Performance standards for antimicrobial susceptibility testing: fifteenth informational supplement M100-S15. CLSI, Wayne
- Crossley KB, Jefferson KK, Archer GL, Fowler VG (2009) *Staphylococci* in human disease, 2nd edn. Blackwell, West Sussex
- Das MC, Paul S, Gupta P, Tribedi P, Sarkar S, Manna D, Bhattacharjee S (2016) 3-Amino-4-aminoximidofurazan derivatives: small molecules possessing antimicrobial and anti-biofilm activity against *Staphylococcus aureus* and *Pseudomonas aeruginosa*. *J Appl Microbiol* 120(4):842–859
- Dubois M, Gilles KA, Hamilton JK, Rebers PA, Smith F (1956) Colorimetric method for determination of sugars and related substances. *Anal Chem* 28:350–356
- Flemming HC, Wingender J (2010) The biofilm matrix. *Nat Rev Microbiol* 8(9):623–633
- Gupta P, Sarkar S, Das B, Bhattacharjee S, Tribedi P (2016) Biofilm, pathogenesis and prevention—a journey to break the wall: a review. *Arch Microbiol* 198(1):1–15
- Hall-Stoodley L, Stoodley P (2009) Evolving concepts in biofilm infections. *Cell Microbiol* 11(7):1034–1043
- Johnson LR (2008) Microcolony and biofilm formation as a survival strategy for bacteria. *J Theor Biol* 251(1):24–34
- Joo HS, Otto M (2012) Molecular basis of in vivo biofilm formation by bacterial pathogens. *Chem Biol* 19(12):1503–1513
- Kaplan JB, Ragunath C, Ramasubbu N, Fine DH (2003) Detachment of *Actinobacillus actinomycetemcomitans* biofilm cells by an endogenous β-hexosaminidase activity. *J Bacteriol* 185(16):4693–4698
- Lau PC, Lindhout T, Beveridge TJ, Dutcher JR, Lam JS (2009) Differential lipopolysaccharide core capping leads to quantitative and correlated modifications of mechanical and structural properties in *Pseudomonas aeruginosa* biofilms. *J Bacteriol* 191(21):6618–6631
- Lee JH, Kim YG, Cho MH, Lee J (2014) ZnO nanoparticles inhibit *Pseudomonas aeruginosa* biofilm formation and virulence factor production. *Microbiol Res* 169(12):888–896
- Lowry OH, Rosebrough NJ, Farr AL, Randall RJ (1951) Protein measurement with the Folin phenol reagent. *J Biol Chem* 193:265–275
- Markman JL, Rekechenetskiy A, Holler E, Ljubimova JY (2013) Nanomedicine therapeutic approaches to overcome cancer drug resistance. *Adv Drug Deliv Rev* 65(13):1866–1879
- Mukherjee K, Tribedi P, Mukhopadhyay B, Sil AK (2013) Antibacterial activity of long chain fatty alcohols against *Mycobacteria*. *FEMS Microbiol Lett* 338(2):177–183
- Ojha AK, Baughn AD, Sambandan D, Hsu T, Trivelli X, Guererdal Y, Alahari A, Kremer L, Jacobs WR, Hattful GF (2008) Growth of *Mycobacterium tuberculosis* biofilms containing free mycolic acids and harbouring drug-tolerant bacteria. *Mol Microbiol* 69(1):164–174
- Oldak E, Trafny EA (2005) Secretion of proteases by *Pseudomonas aeruginosa* biofilms exposed to Ciprofloxacin. *Antimicrob Agents Chemother* 49(8):3281–3288
- Ortvist Å, Hedlund J, Kalin M (2005) *Streptococcus pneumoniae*: epidemiology, risk factors, and clinical features. *Semin Respir Crit Care Med* 26(6):563–574
- Pati R, Mehta RK, Mohanty S, Padhi A, Sengupta M, Vaseeharan B, Goswami C, Sonawane A (2014) Topical application of zinc oxide nanoparticles reduces bacterial skin infection in mice and exhibits antibacterial activity by inducing oxidative stress response and cell membrane disintegration in macrophages. *Nanomed Nanotechnol Biol Med* 10(6):1195–1208
- Salem W, Leitner DR, Zingl FG, Schratte G, Prassl R, Goessler W, Reidl J, Schild S (2015) Antibacterial activity of silver and zinc nanoparticles against *Vibrio cholerae* and enterotoxigenic *Escherichia coli*. *Int J Med Microbiol* 305(1):85–95
- Thaya R, Malaikozhundan B, Vijayakumar S, Sivakamavalli J, Jeyasekar R, Shanthi S, Sonawane A (2016) Chitosan coated Ag/ZnO nanocomposite and their antibiofilm, antifungal and cytotoxic effects on murine macrophages. *Microb Pathog* 100:124–132

- Tribedi P, Sil AK (2013) Low-density polyethylene degradation by *Pseudomonas* sp. AKS2 biofilm. *Environ Sci Pollut R* 20(6):4146–4153
- Tribedi P, Sil AK (2014) Cell surface hydrophobicity: a key component in the degradation of polyethylene succinate by *Pseudomonas* sp. AKS2. *J Appl Microbiol* 116(2):295–303
- Tribedi P, Gupta AD, Sil AK (2015) Adaptation of *Pseudomonas* sp. AKS2 in biofilm on low-density polyethylene surface: an effective strategy for efficient survival and polymer degradation. *Bioresour Bioprocess* 2(1):14
- Vasudevan R (2014) Biofilms: microbial cities of scientific significance. *J Microbiol Exp* 1(3):00014
- Vijayakumar S, Vinoj G, Malaikozhundan B, Shanthi S, Vaseeharan B (2015) *Plectranthus amboinicus* leaf extract mediated synthesis of zinc oxide nanoparticles and its control of methicillin resistant *Staphylococcus aureus* biofilm and blood sucking mosquito larvae. *Spectrochim Acta Part A Mol Biomol Spectrosc* 137:886–891
- Vijayakumar S, Malaikozhundan B, Shanthi S, Vaseeharan B, Thajuddin N (2017) Control of biofilm forming clinically important bacteria by green synthesized ZnO nanoparticles and its ecotoxicity on *Ceriodaphnia cornuta*. *Microb Pathog* 107:88–97